*Journal of the European Ceramic Society* **9** (1992) 265–270

# Residual Stress and the Stress–Strain Relation for Mg-PSZ

P. H. J. van den Berg

Centre for Technical Ceramics, P.O. Box 595, 5600 AN Eindhoven, The Netherlands

&

G. de With*‡

Philips Research Laboratories, P.O. Box 80.000, 5600 JA Enidhoven, The Netherlands

(Received 3 June 1991; accepted 10 August 1991)

***Abstract***

*A stress–strain curve for Mg-PSZ was derived. The elastic part of the curve, described by the bulk modulus* B *of 185 GPa, was determined from the elastic properties measured with the pulse-echo method. The critical transformation stress was determined with two different methods, one based on the strength–toughness curve for Mg-PSZ varieties and one based on the amount of surface rumpling near indentations. Both methods yielded a value for the critical transformation stress of 1·1 GPa. To obtain the transformation modulus, giving the slope of the curve for the plastic deformation, residual stress and X-ray measurements were done on ground surfaces which were polished away in small steps. The residual stress was determined with the bend strip method. This resulted in a residual stress profile for Mg-PSZ and a relation between residual stress and phase content. This relation was combined with the flow law,* $Y = Y_0 + \alpha p$, *where* Y *and* p *denote the flow stress and pressure, respectively, and* $Y_0$ *and* $\alpha$ *are material constants. This resulted in a transformation modulus of 44 GPa, indicating significant work hardening. After complete transformation, the deformation is given by the elastic properties of the now mainly monoclinic zirconia.*

*Es wurde eine Spannungs–Dehnungskurve für Mg-PSZ abgeleitet. Der elastische Teil der Kurve, der durch einen Kompressionsmodul* B *von 185 GPa beschrieben wird, wurde aus den elastischen Eigenschaften bestimmt, die mit Hilfe der Puls-Echo-Methode gemessen wurden. Die kritische Umwandlungsspannung wurde mit zwei verschiedenen Verfahren bestimmt, einmal beruhend auf der Festigkeit–Zähigkeitskurve für verschiedene Mg-PSZ und einmal aufgrund des Anteils faltiger Oberflächen im Bereich von Kerben. Beide Verfahren führten zu dem Wert der kritischen Umwandlungsspannung von 1·1 GPa. Um den Umwandlungsmodul, der die Steigung der Kurve der plastischen Verformung wiedergibt zu bestimmen, wurden Eigenspannungs- und Röntgenmessungen an vorgeschliffenen und in kleinen Schritten abpolierten Oberflächen durchgeführt. Die Eigenspannungsmessungen wurden mit Hilfe der Biegeband-Methode bestimmt. Es ergibt sich ein Eigenspannungsprofil für Mg-PSZ und eine Beziehung zwischen Eigenspannung und Phasenanteil. Diese Beziehung wurde mit einem Fließ gesetz des Typs* $Y = Y_0 + \alpha p$ *in Verbindung gebracht, wobei* Y *der Fließspannung,* p *dem Druck und* $Y_0$ *und* $\alpha$ *Materialkonstanten entsprechen. Es ergibt sich eine Umwandlungsspannung von 44 GPa, was auf eine erhebliche Verfestigung hinweist. Nach vollständiger Umwandlung wird die Verformung durch die elastischen Eigenschaften des nun hauptsächlich monoklinen Zirkoniumoxids beschrieben.*

*Nous avons établi une courbe contrainte–déformation pour une céramique zircone partiellement stabilisée par Mg. La partie élastique de la courbe, décrite par un module élastique* B *d'une valeur de 185 GPa, a été déterminée à partir des propriétés élastiques mesurées par échographie ultrasonore. La contrainte de transformation critique a été déterminée par deux méthodes différentes, une basée sur la courbe résistance–ténacité pour des variétés de Mg-PSZ et*

* To whom all correspondence should be addressed.
‡ Also affiliated with the Centre for Technical Ceramics.



*Journal of the European Ceramic Society* 0955-2219/92/$5.00 

*l'autre, basée sur l'importance de la surface marquée par les indentations. Les deux méthodes conduisent à une valeur de 1·1 GPa. Pour obtenir le module de transformation, donnant la pente de la courbe pour la déformation plastique, on a effectué des mesures de contrainte résiduelle et des clichés RX sur des surfaces polies par étapes successives. La contrainte résiduelle a été déterminée par une mesure en flexion. On en a déduit un profil de contrainte résiduelle pour Mg-PSZ et une relation entre la contrainte résiduelle et la quantité de phase. Cette relation a été combinée avec la loi d'écoulement,* $Y = Y_0 + \alpha p$, *où* Y *et* p *représentent respectivement la contrainte d'écoulement et la pression,* $Y_0$ *et* $\alpha$ *des constantes du matériau. On en déduit un module de transformation de 44 GPa, indiquant un durcissement par écrouissage significatif. Après transformation complète, la déformation est donnée par les propriétés élastiques de la zircone, alors principalement monoclinique.*

## 1 Introduction

Magnesium partially stabilized zirconia (Mg-PSZ) is a commercially available ceramic often investigated.[1-7] The main characteristic of this material is the transformation of tetragonal zirconia into monoclinic zirconia. This phase transformation causes the high toughness of this material, due to the associated dilatation. The phase transformation has been described thoroughly in crystallographic terms,[2-4] but the description in mechanical terms is not yet clear. In general,[5,6] a stress–strain curve as shown in Fig. 1 is presented.

The first part of the curve is determined by the elastic properties of the Mg-PSZ. In a hydrostatic stress state, the elastic deformation is given by the slope of the curve, also referred to as the bulk modulus $B$. The transformation to the monoclinic phase starts after a threshold stress[7,8] has been reached. This threshold is referred to as the critical transformation stress, $\sigma_c$. The description of $\sigma_c$ in terms of the principal stresses is, however, not clear. Its value depends on the stress state, but the quantitative relation is not known.

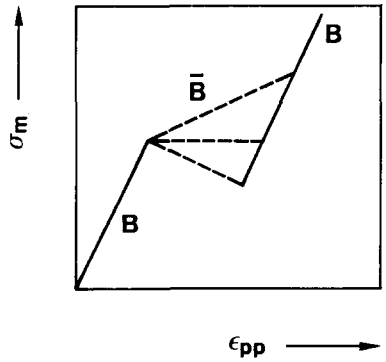


**Fig. 1.** Illustration of the three possible stress–strain curves for Mg-PSZ, where $\sigma_m$ is mean stress, $\varepsilon_{pp}$ is the dilatational strain, $B$ is the clastic bulk modulus and $\bar{B}$ is the transformation bulk modulus.

The slope of the second part of the curve, given by the transformation modulus $\bar{B}$ in a hydrostatic stress state (or more generally by the work-hardening coefficient in other stress states), is still uncertain. Some authors[9,10] have determined part of the curve experimentally for different stress states. Their results clearly indicate work hardening with a work-hardening coefficient that depends on the stress state.

The third part of the curve, starting when all transformable tetragonal zirconia has been transformed into monoclinic, is determined by the elastic properties of mainly monoclinic zirconia. Failure of the material occurs, either by fracture or by plastic deformation of the monoclinic zirconia.

This study presents a different approach to the determination of the slope of the second part of the curve. The stress–strain curve for a biaxial stress state is determined from experimental data. The stress profile and the amount of monoclinic zirconia are measured. Combining the stress data and phase data gives a quantitative relation between the cause, the transformation of tetragonal zirconia to monoclinic zirconia, and the consequence, the residual stress, which is equivalent to the flow stress. The dilatation, $\varepsilon_{pp}$, associated with the complete transformation, is about 4%. The flow stress and $\varepsilon_{pp}$ can thus be related. A flow law from literature[8] relates flow stress to hydrostatic pressure, $p$, so $\varepsilon_{pp}$ and $p$ can be related and an estimate of $\bar{B}$ can be given. The resultant curves are compared with data given in the literature.[9,10]

## 2 Experimental

Commercially available Mg-PSZ was delivered in tiles of about $100 \times 100 \times 10$ mm. Samples were sawn and ground to the required size. All grinding was done as carefully as possible under the same conditions.

The elastic parameters $E$ and $\nu$ were measured with the pulse-echo method on seven samples. Longitudinal waves at 5 MHz and transverse waves at 20 MHz were used. No correction for damping was applied. The fracture toughness of the material was measured with three-point bend tests on 20 single notched samples and with the double can-

tilever beam (DCB) method on three samples. The strength of the Mg-PSZ was determined from 36 samples of 1 × 3 × 15 mm with ground surfaces. The samples were measured and broken in a three-point bend test with the ground surface under tension. The three-point bend tests were performed at a dew point of −40°C, using a span width of 12 mm and a strain rate of about 1·2%/min.

Vickers indentations were made with a Leitz hardness tester at a load of 20 N. The indentations and the surrounding areas were observed with optical microscopy using interference contrast. The indentation diagonal and the radii of the uplifted areas around the indentations (surface rumpling) were measured from photographs.

The residual stress analysis was performed on bend-strip samples. These strips were sawn and ground to dimensions of about 40 × 10 × 1 mm. One surface of 40 × 10 mm was polished until at least 30 μm had been removed from the surface. This side is assumed to represent the bulk material. The strips were glued with the polished side on a 10 mm thick $Al_2O_3$ base. The surface opposite to the polished surface was ground until the strip had a total thickness of somewhere between 0·15 and 0·4 mm. Some of these strips were released from their substrate, after which they curved. Residual glue and dirt were removed in boiling ethanol and/or in a ultrasonic bath with acetone. After this, the curvature of the strip was measured optically.

Other strips were used to determine the stress as a function of depth, measured from the surface. The ground surfaces were polished until a certain amount of surface had been removed (e.g. 5 μm, 10 μm, etc.). Then these strips were also removed from their base, cleaned and measured.

The thickness of a strip was measured with a thickness gauge (Heidenhain, MT30, VT103) at regular positions on the strip. The accuracy of the instrument was ± 1 μm.

The phase content of these bend-strip samples was determined from X-ray analysis, using Cu-$K_\alpha$. The required peak areas were measured from diffractograms with the help of a digitizer coupled to a personal computer.

## 3 Results

The results are summarized in Table 1. The bulk modulus $B$ was calculated from

$$B = E/3(1 - 2\nu) \tag{1}$$

The values obtained are typical of Mg-PSZ.[8,11,12]

**Table 1.** Results of measurements: $2b$ is the diameter of the area of surface rumpling, and $d$ is the indentation diagonal (the values are given as $X \pm S$, where $X$ is the average and $S$ is the sample standard deviation

| | |
|---|---|
| Material properties | |
| Density (g/cm$^3$) | 5·73 ± 0·01 |
| Grain size (μm) | 50 |
| Elastic constants | |
| $E$ (GPa) | 195·0 ± 3·0 |
| $\nu$ | 0·324 ± 0·005 |
| $B$ (GPa) | 185 ± 8 |
| Strength, fracture toughness and indentation dimensions | |
| $\sigma_{3pb}$ (MPa) | 915 ± 56 |
| $K_{Ic}$ (MPa m$^{1/2}$) | |
| DCB | 10·3 ± 0·2 |
| 3pb | 11·5 ± 1·1 |
| $2b$ (μm) | 15·3 ± 2·7 |
| $d$ (μm) | 5 |

| Bend strip results | |
|---|---|
| Depth interval (μm) | Calculated stress average (GPa) |
| 0–2 | 3·2 |
| 2–10 | 0·25 |
| 10 22·5 | 0·1 |
| Depth interval (μm) | Averaged monoclinic zirconia content (%) |
| 0–2 | 92 |
| 2–2·5 | 47 |
| 2·5–6 | 29 |
| 6–8 | 22 |
| 8–10 | 20 |

The critical transformation stress, $\sigma_c$, was determined with two different methods. Firstly, according to the method given in Ref. 8, the indentation diagonal, the Vickers hardness and the radius of surface rumpling were used to determine $\sigma_c$. Secondly, the strength and fracture toughness were used to determine $\sigma_c$ according to the method given in Ref. 12. Both methods gave a value for $\sigma_c$ of about 1·1 GPa. This value of the critical transformation stress depends on the stress state, but the relationship is not clear. The value derived here applies to an approximately hydrostatic stress state.

The residual stress is calculated from the curvature of the bend-strips. There are slight variations in the formulas used.[13–16] Initially eqn (2), from Ref. 15, was used, which was derived for situations in which the strip is clamped to a base to inhibit bending when the residual stress is developed. Afterwards, the strip is released from its base and allowed to curve.

$$S = \frac{E(t + d)^3}{6rdt(1 - \nu)} \tag{2}$$

In this equation, $t$ is the thickness of the substrate, $d$ is the thickness of the residual stress layer, $r$ is the radius of the strip and $S$ is the stress. This formula assumes a constant compressive stress along $d$ and a constant tensile stress along $t$. The arm of the

moment causing the bending of the strip is therefore taken as $(t+d)/2$. The factor $1-v$ is added to account for the biaxial stress state.

The value for $d$, about 22·5 $\mu$m, was determined from the sample that had no clear curvature after 25 $\mu$m had been removed by polishing and the sample which still curved after 20 $\mu$m was removed.

The stress profile for Mg-PSZ calculated from the measurements using eqn (2) gives an exponentially shaped profile with a very high stress at the surface. However, a problem occurred because applying eqn (2) results in stress values that depend on the thickness of the strip. A dependence of the calculated stress on the ratio of $d/t$ is also mentioned in Ref. 16. This problem was solved by adjusting eqn (2) to eqn (3) which takes approximately into account the exponential shape of the stress profile:

$$S = \frac{E(t+d)^3}{12rd((t/2)+d)(1-v)} \tag{3}$$

The arm of the moment causing the bending is now taken as $(t/2)+d$. The error caused by the assumption that the stress is concentrated precisely at the surface, instead of about 1·5 $\mu$m below the surface, is minor and neglected. Applying eqn (3) gives stress data which are not a function of the thickness of the strip but show a normal statistical scatter around an average, The results calculated with eqn (3) are integrated values. The stress–depth results were derived from these values and are shown in Table 1. The profile is illustrated in Fig. 2.

Determination of the amount of monoclinic

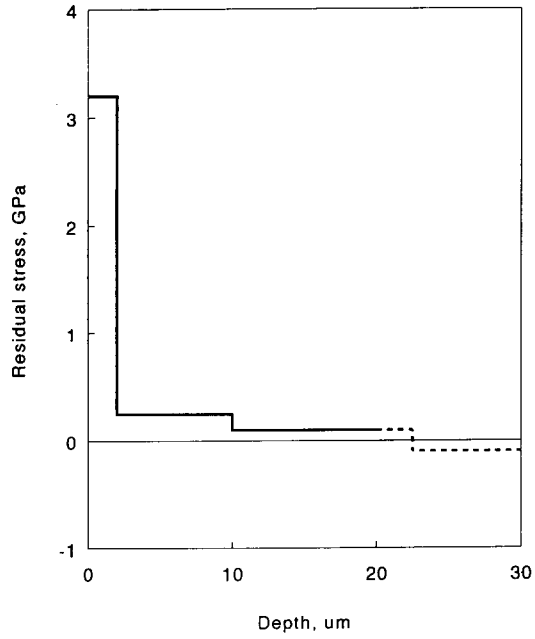


**Fig. 2.** Results of the residual stress analysis. The stress is determined from bending in a plane-stress situation caused by the grinding process.

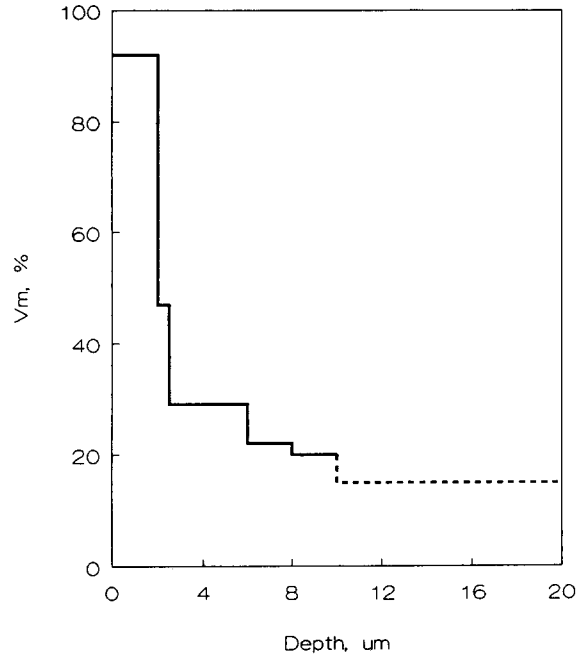


**Fig. 3.** Results from the phase analysis. The amount of monoclinic zirconia, as derived from the measurements done on the bend-strip samples is given as a function of depth. (Transformable tetragonal is transformed into monoclinic zirconia due to the grinding process.)

zirconia in the ternary system (cubic, tetragonal and monoclinic) is problematic. The formula for the binary system, using X-ray analysis, is not without discussion,[17–24] but the best approximation is given by Ref. 17. The usual approach for the ternary system is to replace the tetragonal peak intensity in the formula used for the tetragonal–monoclinic system by the summation of the tetragonal and cubic peak intensity. This is possible because the tetragonal and cubic peak overlap significantly in the $2\theta$ range of interest. This results in:[17]

$$f = 2{\cdot}374I(11\bar{1})_m/(2{\cdot}374I(11\bar{1})_m + I(111)_{c+t}) \tag{4}$$

where $f$ is the volume fraction of monoclinic zirconia and $I$ stands for the area under the peak in question. The values calculated with eqn (4) are also the integrated values. The effective penetration depth of Cu-$K_\alpha$ is about 10 $\mu$m. No difference was measured in the amount of monoclinic zirconia, between a sample from which 30 $\mu$m was removed from its surface through polishing, and a sample from which 10 $\mu$m was removed. The resulting values are given in Table 1 and the profile is shown in Fig. 3, where $V_m = 100f$.

## 4 Discussion

The residual stress is directly related to the flow stress of the transformation plasticity and is referred

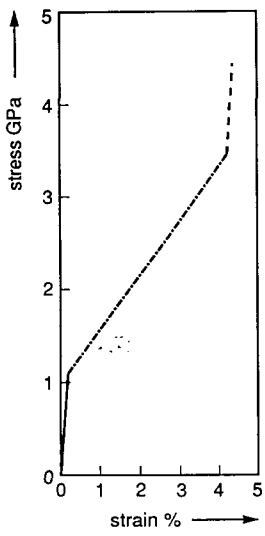


**Fig. 4.** The stress–strain curve as derived from the residual stress analysis and the phase analysis. The elastic bulk modulus in the third part, $B'$, which is the modulus of almost pure monoclinic zirconia, is also taken arbitrarily as about 185 GPa. ——, elastic $B = 185$ GPa; — · —, plastic $\bar{B} = 44$ GPa; – –, elastic $B' = 185$ GPa.

to as $\sigma_f$. Comparing the stress and phase profile as shown in Figs 2 and 3 results, after a correction for the apparent amount of cubic zirconia and non-transformable tetragonal zirconia (8%), in:

$$\sigma_f = 3{\cdot}5f \tag{5}$$

where $\sigma_f$ is in GPa.

The dilatation associated with complete transformation is 4%. This means that $f = 25\varepsilon_{pp}$. Combining with eqn (5) and adding a $\sigma_c$ of 1·1 GPa gives the constitutive equation:

$$\sigma_f = 1{\cdot}1 + 88\varepsilon_{pp} \tag{6}$$

In this case, a $\sigma_c$ of 1·1 Gpa can be used becasue the stress state considered is hydrostatic.

In Ref. 8 the flow law:

$$Y = Y_0 + \alpha p \tag{7}$$

is proposed, where $Y$ is the flow stress, $Y_0$ is the initial flow stress, $\alpha$ is a constant and $p$ is the confining pressure. The predictions about the radius of surface rumpling relative to the indentation size, made by the model associated with eqn (7), correspond to the observations on Mg-PSZ. The constant $\alpha$ was determined from the graphs given in Ref. 8 and the properties of the Mg-PSZ. This resulted in a value for $\alpha$ of 2. Thus, relating eqns (6) and (7), gives:

$$p = 44\varepsilon_{pp} \tag{8}$$

which describes the second part of the hydrostatic stress–strain curve.

After complete transformation, with a strain of 0·04, the material will deform elastically. It is assumed that the bulk modulus of mainly monoclinic zirconia is not significantly different from 185 GPa. The complete curve resulting from this analysis is shown in Fig. 4.

## 5 Considerations

The result of a stress–strain curve showing a significant amount of strain hardening seems to be in contradiction with the observed spontaneous transformation in TEM samples. Phase analysis of HF-etched samples also shows the spontaneous transformation of tetragonal zirconia into monoclinic zirconia. The amount of monoclinic zirconia increases with increasing etching time.

Both these observations of spontaneous transformation are made on samples practically without mechanical constraints. A TEM sample is extremely thin, and HF etching removes material from the surface, leaving unconstrained grains. The Mg-PSZ as examined in this study is a completely dense material. Assume, for example, a sample which has 50% monoclinic zirconia at its surface. There will thus be a compressive stress of 1·8 GPa at this surface according to eqn (5), assuming equibiaxial stress. To transform more zirconia, the critical transformation stress is required to nucleate the transformation, and the compressive residual stress of 1·8 GPa has to be overcome, resulting in a transformation stress of $\sigma_c + 1{\cdot}8$ GPa. This corresponds to significant work hardening.

Comparison with the experimentally measured curves in Refs 9 and 10 illustrates the dependence of $\bar{B}$ on the stress state. The curve given in Ref. 9 is derived from bending in a DCB geometry. Extrapolating the second part of the curve gives a stress of 3·6 GPa at a strain of 4%. This corresponds very well with the value of 3·5 GPa derived from the bend-strip analysis. Both stresses are derived from bending caused by comparable stress states (plane stress). From Ref. 10, a differential stress of 2·3 GPa is determined at 4% axial compressive strain at a confining pressure of 120 MPa. This value is larger than the stress calculated from $p = 44\varepsilon_{pp}$, which at 4% strain is 1·8 GPa. This hydrostatic stress state could give a lower limit to the stress. These numbers illustrate the importance of a clear definition of the stress state, which is also relevant to the value of the critical transformation stress. The hydrostatic stress state could represent one limiting situation, while the biaxial stress state could represent another limiting situation.

The consistent results of this study justify the use of the phase relation (eqn (4)). The direct relation between residual stress and amount of monoclinic zirconia means that a phase analysis gives enough information to describe the residual stress. Research is being done to investigate whether this also holds for other grinding methods, and whether there are significant differences in the residual stress profiles due to different grinding methods.

## 6 Summarizing Conclusions

—The results from the X-ray analysis and the bend-strip measurements indicate a clear relationship between the phase transformation and the residual stress.

—The present results lead to the stress–strain curve shown in Fig. 4, which illustrates the importance of strain hardening for the deformation of this material.

—The values of the critical transformation stress, $\sigma_c$, the transformation bulk modulus, $\bar{B}$, and the work-hardening coefficient depend on the stress state.

—The results of a phase analysis can be directly related to the residual stress for the grinding process applied. Further work is being done to investigate whether this can be extrapolated to various other surface treatments.

## References


1. Evans, A. G., Perspective on the development of high-toughness ceramics. *J. Am. Ceram. Soc.*, **73** (1990) 187.
2. Evans, A. G. & Heuer, A. H. J., Review—transformation toughening in ceramics: martensitic transformations in crack-tip stress fields. *J. Am. Ceram. Soc.*, **63** (1980) 241.
3. Lee, R.-R. & Heuer, A. H., In-situ martensitic transformation in a ternary $MgO$–$Y_2O_3$–$ZrO_2$ alloy: I, transformation in tetragonal $ZrO_2$ grains. *J. Am. Ceram. Soc.*, **71** (1988) 694.
4. Chaim, R. & Brandon, D. G., Microstructure evolution and ordering in commercial Mg-PSZ. *J. Mater. Sci.*, **19** (1984) 2934.
5. Budiansky, B., Hutchinson, J. W. & Lambropoulos, J. G., Continuum theory of dilatant transformation toughening in ceramics. *Int. J. Solids Structure*, **19** (1983) 337.
6. Evans, A. G. & Cannon, R. M., Toughening of brittle solids by martensitic transformations. *Acta Met.*, **34** (1986) 761.
7. Heuer, A. H. & Rühle, M., On the nucleation of the martensitic transformation in zirconia. *Acta Met.*, **33** (1985) 2101.
8. Chen, I.-W., Implications of transformation plasticity in $ZrO_2$-containing ceramics: II, Elastic–plastic indentations. *J. Am. Ceram. Soc.*, **69** (1986) 181.
9. Ingels, E., Heuer, A. H. & Steinbrech, R. W., Fracture mechanics of high-toughness magnesia-partially-stabilized-zirconia. *J. Am. Ceram. Soc.*, **73** (1990) 2023.
10. Chen, L.-W. & Morel, P. E. R., Transformation plasticity and transformation toughening in Mg-PSZ and Ce-TZP. In *Mat Res. Soc. Symp. Proc.*, **78** (1987) 75, *Advanced Structural Ceramics*, ed. P. F. Becker, M. V. Swain & S. Somiya.
11. Swain, M. V., Garvie, R. C. & Hannink, H. J., Influence of thermal decomposition on the mechanical properties of magnesia-stabilized cubic zirconia. *J. Am. Ceram. Soc.*, **66** (358) 1983.
12. Swain, M. V., Inelastic deformation of Mg-PSZ and its significance for strength-toughness relationship of zirconia toughened ceramics. *Acta Met.*, **33** (1985) 2083.
13. Samuel, R. & Chandrasekar, S., Effect of residual stresses on the fracture of ground ceramics. *J. Am. Ceram. Soc.*, **72** (1989) 1960.
14. Treuting, R. G. & Read, Jr, W. T., A mechanical determination of biaxial residual stress in sheet metals. *J. Appl. Phys.*, **22** (1951) 130.
15. Brenner, A. B. & Senderoff, S., Calculation of stress in electrodeposits from the curvature of a plated strip. *J. Research*, **42** (1949) 105.
16. Chiu, C.-C., Determination of the elastic modulus and residual stresses in ceramic coatings using a strain gage. *J. Am. Ceram. Soc.*, **73** (1990) 1999.
17. Evans, P. A., Stevens, R. & Binner, J. G. P., Quantitative X-ray diffraction analysis of polymorphic mixes of pure zirconia. *Brit. Ceram. Trans. J.*, **83** (1984) 39.
18. Toraya, H., Yoshimura, M. & Somiya, S., Calibration curve for quantitative analysis of the monoclinic-tetragonal $ZrO_2$ system by X-ray diffraction. *Comm. Am. Ceram. Soc.*, (1984) C-119.
19. Garvie, R. C. & Nicholson, P. S., Phase analysis in zirconia systems. *J. Am. Ceram. Soc.*, **55** (1972) 303.
20. Schmid, H. K. J., Quantitative analysis of polymorphic mixes of zirconia by X-ray diffraction. *J. Am. Ceram. Soc.*, **70** (1987) 376.
21. Garvie, R. C., Hannink, R. H. and Pascoe, R. T., Ceramic steel? *Nature*, **258** (1975) 703.
22. McCullough, J. D. & Trueblood, K. N., The crystal structure of baddeleyite (monoclinic $ZrO_2$). *Acta Cryst.*, **12** (1959) 507.
23. Smith, D. K. & Newkirk, H. W., The crystal structure of baddeleyite (monoclinic $ZrO_2$) and its relation to the polymorphism of $ZrO_2$. *Acta Cryst.*, **18** (1965) 983.
24. Porter, D. L. & Heuer, A. H., Microstructural development in MgO-partially stabilized zirconia (Mg-PSZ). *J. Am. Ceram. Soc.*, **62** (1979) 298.